Proceedings of the 9th U.S. National and 10th Canadian Conference on Earthquake Engineering
Compte Rendu de la 9ième Conférence Nationale Américaine et
10ième Conférence Canadienne de Génie Parasismique
July 25-29, 2010, Toronto, Ontario, Canada • Paper No 528

PREDICTION OF M_W=6.2 KOJOOR EARTHQUAKE IN NORTH OF IRAN, USING EMPIRICAL GREEN FUNCTIONS

Ali Golara[1], Roohollah Ahmady Jazany[2], Hossein Kayhani[3]

ABSTRACT

In this paper potential use of the EGF (empirical green function) approach as a prediction tool in strong ground motion seismology is presented. This analysis was carried out on Kojoor earthquake. Here thirty possible rupture models are generated on causative fault's plane to account for source variability. These models were based on previous study of this area and without including any knowledge of the source characteristics prior to the occurrence of this earthquake. The strong ground motion prediction provides an accurate, justifiable means to characterize site and path effects, and therefore allows the uncertainties in the predicted hazard to be because of unresolved issues about the earthquake source such as the geological constraints of a particular fault and details about the physics of earthquakes. It is found that the actual ground motion recordings fell within the range of synthesized ground motions. To conclude, it is possible to make reasonable strong ground motion "predictions" even without having an extensive knowledge of the fault characteristics using proposed methodology.

Introduction

In recent years, seismologists have attempted to develop quantitative models of earthquake rupture process with the ultimate goal of predicting strong ground motion. The idea of studying large earthquakes by means of seismograms of small earthquakes, used as empirical Green's function (EGF), was introduced initially by Hartzell (1978). Later methods proposed by Irikura (1983), Joyner & Boore (1986), Boatwright (1988), Wennerberg (1990), Hutchings et al (1990), are modifications of EGF's method. In empirical Green's function approach, rupture propagation and radiation pattern were specified deterministically and the source propagation and

[1] MSc Graduate, International Institute of Earthquake Engineering and Seismology (IIEES), Tehran, Iran, and *Master of Crisis* and Disaster *Management in Ministry* of *Petroleum* of Iran (Responsible for Crisis Room in Iranian Gas Company)
[2] PhD Candidate, Structural Research Centre, International Institute of Earthquake Engineering and Seismology (IIEES),Tehran, Iran
[3] PhD Candidate, Science and Research Branch, Islamic Azad University, Tehran, Iran

radiation effects were included empirically by assuming that the motions observed from aftershocks contained this information (Somerville et al., 1991).

The EGF methods can be used in both inverse and direct problems. In the inverse problems, EGF method help to retrieve the focal mechanism and the source time function, to determine the moment tensor, or to find the rupture parameters or the slip distribution on fault (Mueller, 1985; Mori and Frankel, 1990; Hutchings, 1991; Courboulex et. al., 1997). In direct problems, EGF method can be used as a predicting tool in strong ground motion seismology as developed by Irikura, 1983; Joyner and Boore, 1986; Boatwright, 1988; Tumarkin et al., 1994; Hutchings (1991 and 1994).

In this study, we tested the potential of EGF approach usage as a predicting tool in strong ground motion prior to an earthquake and with little information about the future rupture process. To test this idea, we analyzed the May 28, 2004, $M_w = 6.2$ Kojoor Earthquake, North of Iran. The main shock, which occurred about 70 kms north of Tehran and at a similar distance to another metropolitan area caused little loss but it was felt severely at a radius of over about 200 kms.

Thirty possible earthquake scenarios were randomly generated for Kojoor fault. We tested if synthesized ground motions have a range that span the observed records for the 2004 Kojoor earthquake. In this situation, the rupture parameters were randomly allowed to vary within a larger range to encompass the parametric uncertainty. In this paper, we only consider linear ground motion response. The records were used in the study occurred on geologically competent or low enough values to be considered as a linear response.

Methodology

The summation of the small events (EGFs) is thus based on scaling relations between small and large events. The number of sub events or EGFs is N^3, where the scaling parameter N is an integer value determined as the ratio of the moment of the target event to the moment of the small event. Because this number is relatively small, the discretization of the rupture process is quite coarse, which produces high-frequency spatial and temporal aliasing effects (Bour & Cara 1997). On the other hand, a lack of high-frequency content above the corner frequency of the EGFs results in deficiencies in the high-frequency part of the large event. Therefore, some approaches (e.g.Wennerberg1990) use random summation to artificially generate high frequencies.

In contrast, 'the rupture parameter approach '(Hutchings 1991) requires very small events ($M0<1.5\times1014$ N.m), for which scaling relations are not valid. By deconvolving the assumed source time function and normalizing the time-series of the small earthquake with its moment, records of the these events can be used directly in the representation relation (Aki& Richards 1980) as empirical Green's function as shown by Hutchings & Wu (1990). The actual rupture process is simulated by adding up EGFs using a kinematic rupture model. Therefore, the fault plane of the target event is discretized into elemental areas that are small enough to model continuous rupture up to the highest frequency of interest. The sum of the moments of all elements matches any arbitrary given target moment.

There were not enough small events available to provide the empirical Green's functions because of poor signal to noise ratios. Therefore, moderate-size earthquakes were used to provide empirical Green's functions. Impulsive point source empirical Green's functions were created

from these moderated size events by deconvolving out a Brune source. In this paper, Green's functions for each portion of the fault are calculated and convolved with source functions at each point along the rupture surface. Here, we use empirical Green's functions and synthesized ground motion from 0.3 to 30.0 Hz, Because of availability and better signal to noise for recorded earthquake. Figure 1 shows three recordings that were corrected to provide effective impulsive and point shear source event recordings (EGFs).

Strong Ground Motion Data

The main Kojoor earthquake was recorded by 138 stations. Digitized three-component recordings from this earthquake were obtained from building & housing research center (BHRC). Only three stations were considered in this study because they are the only ones that have recorded both the main shock and aftershocks. Therefore, in this study the observed records were synthesized at *Pool*, *Noor*, *Noshahr* stations for three components. Observed records in three components at Pool, Noor and Noshahr stations for the main Kojoor earthquake are shown in figure 1. Table 1 lists the salient feature of these three stations. The Peak ground acceleration (PGA) of the records used in this study ranged from 0.02 to 0.11 g for these three stations except Pool, which had 0.29 g PGA, are in the linear response range. Station Pool is on alluvial site and furthermore, the observation that its records are modeled as well as other stations suggests that it has not had non-linear response.

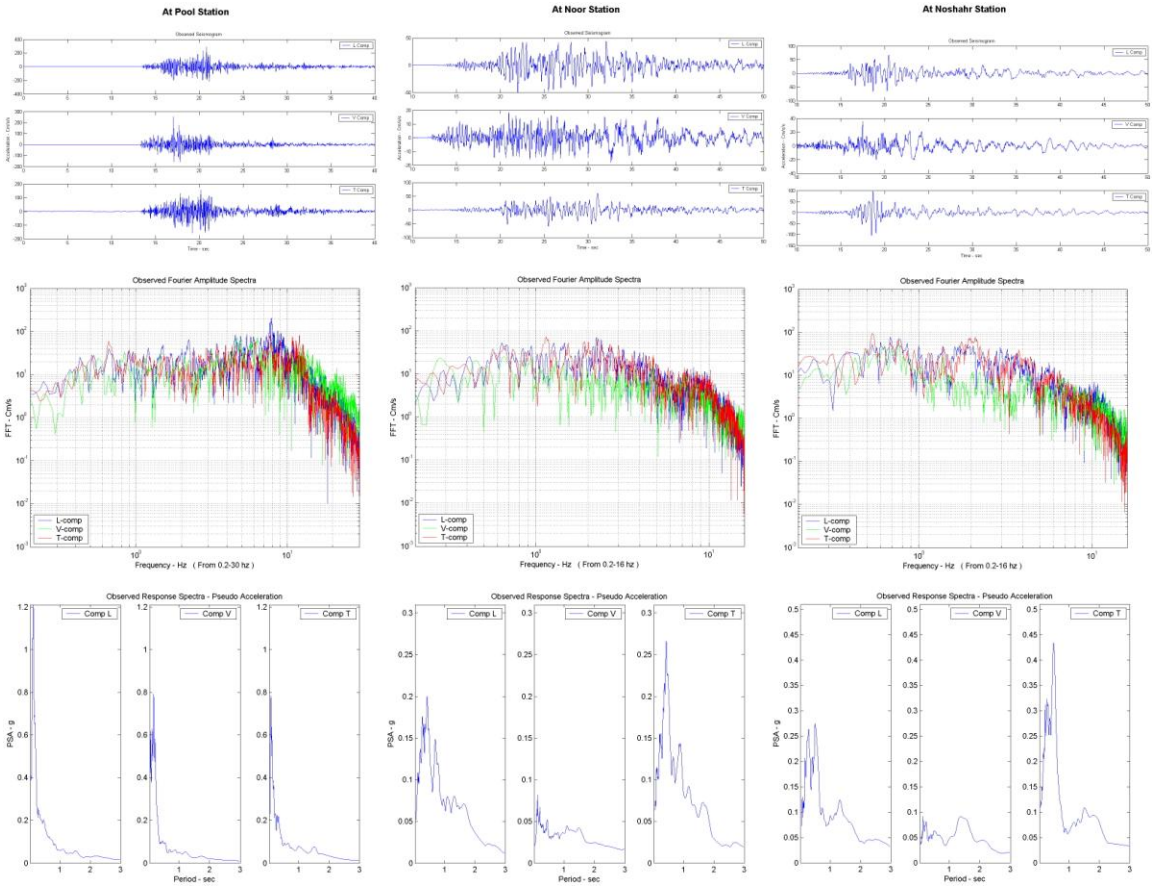

Figure 1. Observed time-series, Fourier and pseudo acceleration response spectra in three

components at Pool, Noor and Noshahr station for the main Kojoor earthquake.

The first aftershock was recorded about 2 minutes after the main shock with the PGA of 0.012g at the Pool station. The largest aftershock occurred at 13:53:51 local time on May 29, 2004 (M_b=5 and with M_w=4.8 and it is shown in Table 2). This aftershock also has been recorded by Pool station accelerograph with the PGA of 0.083g.

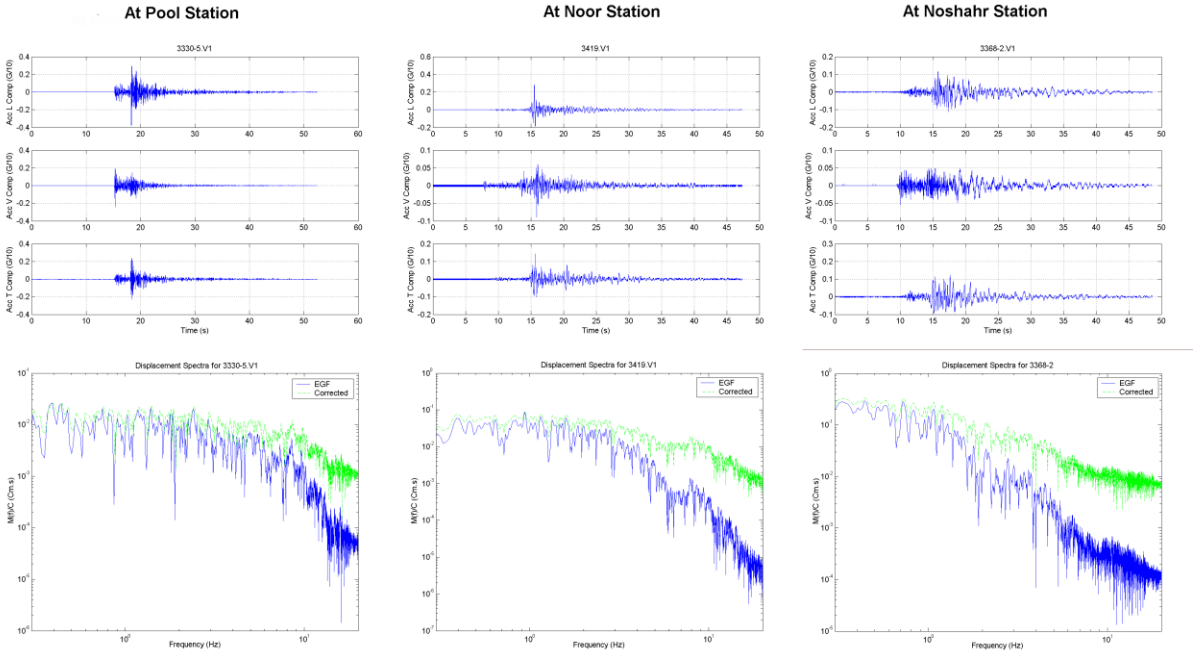

Figure 2. Recorded seismograms and spectra (identified by EGF) and results after the Brune source model have been deconvoled (identified by "corrected") at Pool, Noor, and Noshahr stations, respectively.

Table 1: Coordinate of stations which have recorded both the main shock and aftershocks, hypocentral distance of main shock, azimuth of two horizontal components, and their Geol. Class

Station	No. EGF with 4<M<5	Geographical Coordinates		Hypocentral Distance (km)	Azimuth		Geol. Class
		E	N		L	T	
Pool	7	51.72	36.38	18	220	310	Group 2
Noor	4	52.02	36.57	45	355	85	Group 3
Noshahr	2	51.5	36.65	40	112	202	Group 3

Table 2: Hypocentral coordinates and source parameters such as corner frequency, moment magnitude, and site-specific for the EGF's

Pool Station recorded event ID	Lat. (◦)	Long. (◦)	Depth (km)	f_c (Hz)	M_w	κ_g ,	κ_g ,

						Hori.Comp.	Ver. Comp.
040528131507	36.45	51.59	37	2.8	4.6	0.03	0.019
040528133556	36.40	51.61	28	3.1	4.4	0.025	0.0208
040528194705	36.37	51.45	28	1.3	4.8	0.041	0.031
040529092351	36.41	51.35	28	1.2	4.8	0.026	0.019
040530014241	36.40	51.61	28	1.9	4.5	0.032	0.02
040530192702	36.42	51.66	10	2.1	4.6	0.034	0.0227
040607040123	36.41	51.51	28	1.5	4.1	0.02	0.028
Noor Station recorded event ID	Latitude	Longitude	Depth	f_c (Hz)	M_w	κ_g , Hori. Comp.	κ_g , Ver. Comp.
040528131507	36.45	51.59	37	1.5	4.6	0.051	0.0327
040529092351	36.41	51.35	28	0.7	4.8	0.053	0.0435
040530014241	36.40	51.61	28	1.4	4.5	0.053	0.04
040530192702	36.42	51.66	10	1.5	4.6	0.056	0.049
Noshahr Station recorded event ID	Latitude	Longitude	Depth	f_c (Hz)	M_w	κ_g , Hori. Comp.	κ_g , Ver. Comp.
040529092351	36.41	51.35	28	0.7	4.8	0.045	0.036
040530014241	36.40	51.61	28	1.1	4.5	0.048	0.035

Strong Ground Motion "Prediction" Analysis

We tried to establish the potential of this rupture parameters approach as a prediction tool in strong ground motion seismology. Golara et al (2006) found that Kojoor fault was the causative fault for this earthquake. Here, a range of possible ground motion was evaluated running some scenarios solely on the Kojoor fault plan. (Region II in Figure 3).

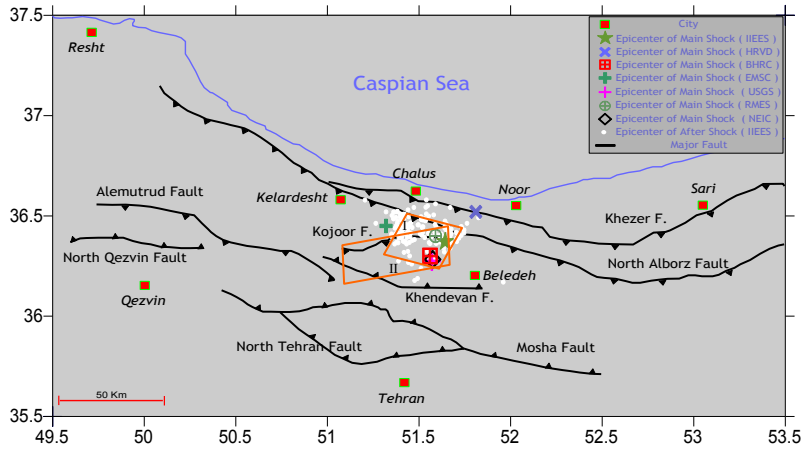

Figure 3. Location of epicenter reported by IIEES, HRVD, EMSC, USGC, RMES, NEIC, and location of aftershocks, and the rectangles are the larger and smaller source zones referred to in the text.

Hutchings et al (2007) synthesized 500 earthquakes that distributed throughout a source volume likely to have M_w=6.0 earthquakes near Athens. They showed that after about 30

scenarios, the mean of predicted data stabilizes and full variability of possible ground motion from this approach have been accounted for. Therefore, we compute some strong ground motion parameters from 30 different random scenarios supposing no previous information regarding the source characteristics of the Kojoor main earthquake are available. Then we tested if the actual ground motion record fell within the range predicted. The rupture surface geometry was chosen as a rectangular with dimension correlated with the magnitude of the earthquake to synthesize (M_w=6.2). The hypocentral location was left free to vary within the hazard area. Input parameters values used for calculating scenarios are displayed in Table 3. Synthetic seismograms were evaluated for each rupture scenario at all stations for all components that would lead to 90 waveforms. The comparisons were based on some ground motion parameters and response spectra at Pool station (soil type 2 and focal distance near 18 km), Noor station (soil type 3 and focal distance near 45 km) and at Noshahr station (soil type 3 and focal distance near 40 km). For estimating the prediction uncertainty, the mean plus one standard deviation of these parameters and spectra was also calculated. The results are shown in Table 4 and Figure 4.

Table 3: The limits of input parameters that are used for prediction of the main Kojoor earthquake

	Rupture parameters
Slip Function	Kostrov with healing
Fault Geometry	Length of rupture 10.0 km ± 5.0 km Width of rupture 8.0 km ± 3.5 km
Focal Mechanism	Strike 100° ±20.0°, dip 30.0° ± 15.0°
Roughness percentage	is selected to be either 0, 10, 20, 33, 55% of fault surface
Moment	(2.3 ± 0.5)*E+25 dyne-cm
Rise Time	Dependent on Vr, Vh and hypocenter location
Shear wave Velocity	3.2 ± 0.3 Km/s
Rupture Velocity	0.8 times the shear wave velocity
Healing Velocity	0.9 times the rupture velocity
Slip Vector	constrained to 68.0° ± 20.0°

Considering Uncertainties

Following the terminology introduced by Abrahamson et al. (1990), two elements should be taken into account for predicting the uncertainties: the parametric uncertainty and the so-called "modeling and random errors". While the first depends on the parameters used and their uncertainties, the second depends on the moment estimates for the EGF's and on the random errors that can affect the interpolation of events along with fault. Concerning the parametric uncertainties, it is important to verify the choice of using just 30 scenarios by randomly varying each parameter that we assume uniformly distributed over its own allowed range and uncorrelated with the others.

Hutchings et al (2003) showed the engineering parameters fit into a lognormal distribution. Therefore, they pass a χ^2 test (Freund, 1962) for the log normal distribution. Here, ground-motion intensity measurement is defined by calculating the PGA, Acc RMS, Duration and

PSA (pseudo acceleration response spectra) values of the synthetic ground motion waveforms, calculated as the average of the log of longitudinal and transverse components and also, as the log of vertical component. However, about PSA in this paper, result is only calculated as the average of the log of longitudinal. Therefore, the estimation of the median (lognormal mean) parameters is:

$$\hat{H}_j = \frac{1}{n}\sum_{i=1}^{n}\log(R_i) \qquad (1)$$

Where, R is one of the engineering parameters. For (PSA), it is calculate for each period. The index i range over the 30 scenarios. Finally, the ranges of engineering parameters for future earthquake are estimated as: $H_j^{\sigma} = \hat{H}_j \pm \sigma$, where: $\sigma^2 = \sigma_p^2 + \sigma_m^2 + \sigma_e^2 + \sigma_r^2$ and σ_p^2 is the variance of the distribution of log(R) for the 30 scenarios. This estimation comes from the uncertainty on which earthquake scenario is likely to occur; σ_m^2 accounts for modeling errors, which comes from the uncertainty of the actual rupture scenarios, and from random errors due to the interpolation of Green's functions and their incorrect moment estimation. These errors, unknown for this study, are assumed to be equal to the standard deviation obtained by Jarpe and Kasameyer (1996), which is 0.0795; σ_e^2 is the variance due to random errors in source parameters of empirical Green's functions; σ_r^2 is the variance of the computation of both the lognormal mean and the standard deviation, and it has a value of 0.0011 (Hutchings et al., 2003).

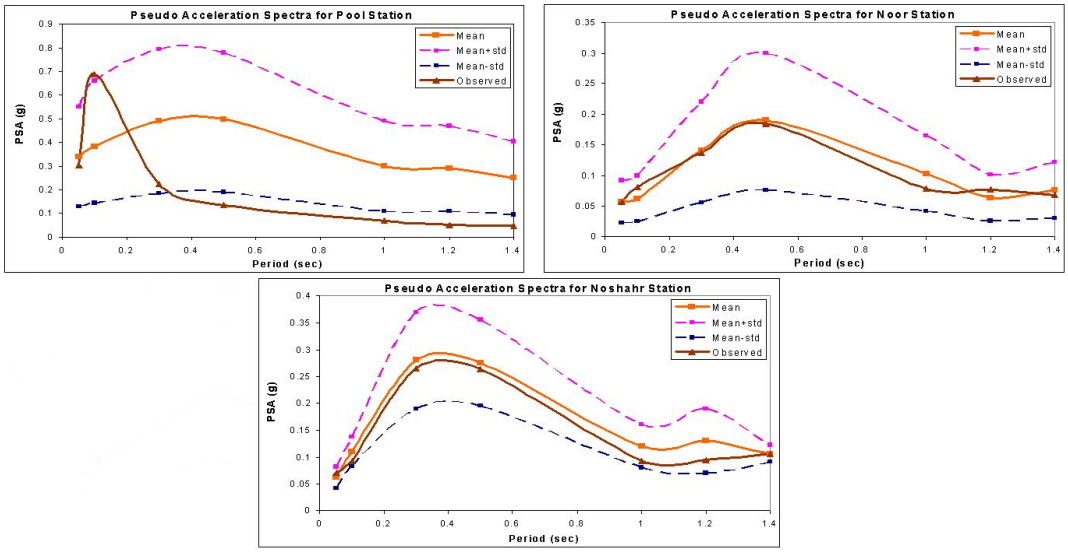

Figure 4. Comparison of pseudo acceleration spectra (for 5% damping) for predicted and observed main earthquake at Pool, Noor, and Noshahr station, respectively.

Though in an authentic prediction tool the comparison between the real and the synthetic strong ground motion is impossible, it was decided to complete the prediction analysis by performing the score evaluation between preferred engineering parameters and response spectra of synthetic seismograms and the actual recordings of the Kojoor main earthquake. As can be seen in Table 4, results demonstrate that the engineering characteristics of actual time series can be captured at each site with a range of possible assumed rupture models. The comparison

between response spectra computed from the synthesized accelerograms and observed response spectra are shown in Figure 4. At Noor and Noshahr stations synthesized response spectra match the observed response spectra very well and at Pool station deviations to higher values are evident in the high-period range (>0.3 sec) by source rupture parameter combinations. However, they partly fit in the σ -standard deviation range.

Table 4: Predicted bands and observed engineering parameters values of the Kojoor earthquake at station of Pool, Noor, and Noshahr

Pool Station	Mean	Mean-std	Observed Value	Mean+std	Validation
PGA (g)-Mean Horizontal Comp.	0.198	0.118	0.228	0.278	Good
PGA (g)-Vertical Comp.	0.13	0.06	0.25	0.2	Bad
Acc RMS (g)-Mean Horizontal Comp.	0.0265	0.0177	0.032	0.0353	Good
Acc RMS (g)-Vertical Comp.	0.019	0.011	0.0153	0.027	Good
Duration (s)-Mean Horizontal Comp.	6.678	4.886	5.0175	8.47	Good
Duration (s)-Vertical Comp.	6.39	4.81	5.235	7.97	Good
Noor Station	Mean	Mean-std	Observed Value	Mean+std	Validation
PGA (g)-Mean Horizontal Comp.	0.0598	0.0266	0.0559	0.093	Good
PGA (g)-Vertical Comp.	0.031	0.011	0.0186	0.051	Good
Acc RMS (g)-Mean Horizontal Comp.	0.0103	0.0099	0.00935	0.0107	Good
Acc RMS (g)-Vertical Comp.	0.00533	0.002652	0.00396	0.008	Good
Duration (s)-Mean Horizontal Comp.	11.099	8.918	11.95	13.28	Good
Duration (s)-Vertical Comp.	13.9692	11.06834	20.88	16.87	Bad
Noshahr Station	Mean	Mean-std	Observed Value	Mean+std	Validation
PGA (g)-Mean Horizontal Comp.	0.096	0.073	0.087	0.119	Good
PGA (g)-Vertical Comp.	0.037	0.031	0.036	0.043	Good
Acc RMS (g)-Mean Horizontal Comp.	0.0232	0.015	0.0122	0.0314	Good
Acc RMS (g)-Vertical Comp.	0.0081	0.0062	0.0053	0.01	Bad
Duration (s)-Mean Horizontal Comp.	10.4	9.01	9.417	11.79	Good
Duration (s)-Vertical Comp.	13.65	12.4	13.57	14.9	Good

Conclusion

The purpose of this investigation was to test the rupture parameter approach proposed by Hutchings (1991). Nevertheless, in this study $4.0<M\leq 5$ events instead of very small events have been used. For this purpose, impulsive point shear source empirical Green's functions have been generated by deconvolving out the source contribution of moderate-size events.

It was decided to use the procedure in its real objective that is a prediction of the ground motion in advance if very little is known about what is going to happen. In this study, thirty possible ground motions scenarios have been developed starting from the main Kojoor earthquake source parameters to see if the actual ground motion recordings fall within the range predicted ones. The comparison have been carried out on engineering parameters and pseudo acceleration spectra (PSA) and by evaluating the match's score between the 90 synthetic seismograms evaluated for each station, and the real records. Generally, it has been found these engineering parameters and the PSA calculated for the Kojoor fall well within the predicted range. It emerges that it is possible to make reasonable strong ground motion "predictions" even without having a deep knowledge of the fault characteristics at least for this main earthquake, by running thirty possible models.

References

Abrahamson, N. A., P.G. Somerville, and C. A. Cornell (1990), Uncertainty in Numerical Strong Motion Predictions, in Proc. *4th U.S. National Conf. Earthquake Engineering*, Vol.1 (Earthquake Engineering Research Institute, 20-24 May, Plam Springs, California).

Aki, K. (1967). Scaling law of Seismic spectrum, Journal Geophysical Research, Vol.72, pp.1217-1231.

Aki, K. and P. G. Richards (1980). Quantitative seismology, Theory and Methods, Volumes I and II, W. H. Freeman and Company, San Francisco, CA.

Boatwright, J. (1988). The seismic radiation from computer models of faulting, Bulletin of the Seismological Society of America, 78, 489-508.

Bour, M. & M. Cara (1997). Test of a simple empirical Green's function method on moderate-sized earthquakes. Bulletin of the Seismological Society of America, 87, 668-683.

Brune, J.N (1970). Tectonic stresses and spectra of seismic wave from earthquake, Journal Geophysical Research, 75, 4997-5009.

Brune, J.N. (1971). Corrections, Journal Geophysical Research, Vol.76, p.5002.

Freund, J.E. (1962). Mathematical Statistics, Pren-tice-Hall, Inc., Englewood Cliffs, N.J, USA: Prentice-Hall, Inc., 16th printing, 1962.

Golara, A. and H. Hamzehloo (2006). Strong ground motion modeling for the 2004 Firozabad-Kojoor earthquake, north of Iran. First European Conference on Earthquake Engineering and Seismology (a joint event of the 13th ECEE & 30th General Assembly of the ESC) Geneva, Switzerland, 3-8

September 2006. Paper Number: 895.

Hartzell, S.H. (1978). Earthquake aftershocks as Green's functions. Geophysical Research Letter,5, 1-4.

Hutchings, L. and F. Wu (1990). Empirical Green's functions from small earthquakes waveform study of locally recorded aftershocks of the San Fernando earthquake, Journal Geophysical Research, 95, 1187-1214.

Hutchings, L. (1991). Prediction of strong ground motion for the 1989 Loma Prieta earthquake using empirical Green's functions, Bulletin of the Seismological Society of America, 81, 88-121.

Hutchings, L. (1994). Kinematic Earthquake Models and Synthesized Ground Motion Using Empirical Green's Functions. Bulletin of the Seismological Society of America, 84, 1028-1050.

Hutchings, Lawrence, P.W. Kasameyer and W. Foxall (2003) LLNL, Hazard Mitigation Center Ground Motion Prediction Methodology. Lawrence Livermore National Laboratory, UCRL-ID 135697.

Hutchings et al. (2007). A Test of a Physically Based, Strong Ground Motion Prediction Methodology with the 7 September 1999, Mw=6.0 Athens Earthquake and Application to PSHA. November 19, 2004, In press, Geophysical Journal International.

Irikura, K. (1983). Semi-empirical estimation of strong ground motions during large earthquakes. Bulletin Disaster Prev. Research Institute (Kyoto University) 33, 63-104.

Jarpe, S.J. and P. K. Kasameyer (1996). Validation of a Methodology for Predicting Broadband Strong Motion Time Histories using Kinematic Rupture Models and Empirical Green's Functions. Bulletin of the Seismological Society of America, 86, pp1116-1129.

Joyner, W. B., and D.M. Boore (1986). On simulation large earthquakes by Green's functions addition of smaller earthquakes, in Earthquake Source Mechanics, (Maurice Ewing series 6), S. Das, J. Boatwright, and C. H. Sholtz (Editors), American Geophysical Monograph 37, Washington, D.C., 269-274.

Mori, J., and A. Frankel (1990). Source parameters for earthquakes associated with the 1986 North Palm Springs, California, earthquake determined using empirical Green functions, Bulletin of the Seismological Society of America, 80, 278-295.

Mueller, C. S. (1985). Source pulse enhancement by deconvolution of an empirical Green's function, Geophysical Research Letter, 12, 33-36.

Somerville, P.G., M. Sen and B. Cohee (1991). Simulation of strong ground motion recorded during the 1985 Michoacan, Mexico and Valparaiso, Chile earthquakes. Bulletin of the Seismological Society of America, 81, 1-27.

Tumarkin, A. G., R. J. Archuleta, and R. Madariaga (1994). Scaling relations for composite earthquake models, Bulletin of the Seismological Society of America, 84, 1279-1283.

Wennerberg, L. (1990). Stochastic summation of empirical Green's functions, Bulletin of the Seismological Society of America, 80, 1418-1432.